0888-8809/02/$15.00/0
Printed in U.S.A.

Molecular Endocrinology 16(1):116–127

Linkage of Rapid Estrogen Action to MAPK Activation by ERα-Shc Association and Shc Pathway Activation

ROBERT X.-D. SONG, ROBERT A. MCPHERSON, LIANA ADAM, YONGDE BAO, MARGARET SHUPNIK, RAKESH KUMAR, AND RICHARD J. SANTEN

Departments of Internal Medicine (R.X.-D.S., R.A.M., M.S., R.J.S.) and Biomolecular Research Facility (Y.B.), University of Virginia School of Medicine, Charlottesville, Virginia 22908; and Department of Molecular & Cellular Oncology (L.A., R.K.), University of Texas M.D. Anderson Cancer Center, Houston, Texas 77030

E2 rapidly activates MAPK in breast cancer cells, and the mechanism for this effect has not been fully identified. Since growth factor-induced MAPK activation involves signaling via the adapter protein Shc (Src-homology and collagen homology) and its association with membrane receptors, we hypothesized that breast cancer cells utilize similar signaling mechanisms in response to E2. In the present study, we demonstrated that E2 rapidly induced Shc phosphorylation and Shc-Grb2 (growth factor receptor binding protein 2)-Sos (son of sevenless) complex formation in MCF-7 cells. Overexpression of dominant negative Shc blocked the effect of E2 on MAPK, indicating a critical role of Shc in E2 action. Using selective inhibitors, we also demonstrated that ERα and Src are upstream regulators of Shc. A rapid physical association between ERα and Shc upon E2 stimulation further evidenced the role of ERα on Shc activation. Mutagenesis studies showed that the phosphotyrosine binding and SH2 domains of Shc are required to interact with the activation function 1, but not activation function 2, domain of ERα. Using a glutathione-*S*-transferanse-Shc pull-down assay, we demonstrated that this ERα-Shc association was direct. Biological consequences of this pathway were further investigated at the genomic and nongenomic levels. E2 stimulated MAPK-mediated Elk-1 transcriptional activity. Confocal microscopy studies showed that E2 rapidly induced formation of membrane ruffles, pseudopodia, and ERα membrane translocation. The E2-induced morphological changes were prevented by antiestrogen. Together our results demonstrate that ERα can mediate the rapid effects of E2 on Shc, MAPK, Elk-1, and morphological changes in breast cancer cells (*Molecular Endocrinology* 16: 116–127, 2002)

E2 IS a steroid hormone that plays an important role in the genesis of human breast cancer and in the growth of established tumors (1). Classically, E2 elicits genomic effects on transcription via ERα and ERβ, which are mainly located in the nucleus. As ligand-dependent transcriptional factors, the hormone-bound ERs interact with estrogen response elements to stimulate certain genes in E2-responsive tissues and to regulate gene transactivation (2). The genomic actions of E2 are characterized by delayed onset of action and sensitivity to inhibitors of transcription and translation. Many of the E2-induced transcriptional mechanisms involve ERα, which can be functionally regulated by posttranslational phosphorylation of serine residues at the 104, 106, 118, 167, and 236 positions (3–6). In addition, tyrosine-537 of ERα has been reported to be phosphorylated in MCF-7 cells and in ERα-expressing Sf9 insect cells (7). The biological function of ERα is also regulated by association with a subset of nuclear proteins, such as coactivators, corepressors, and integrator proteins (8–11).

More recently, investigators have recognized rapid nongenomic actions of E2 on several cellular processes, such as activation of Ras (12), Raf-1 (13), PKC (14), PKA (15), Maxi-K channels (16), increments in intracellular calcium levels (17), and an increase of nitric oxide (17). Elicited responses depend upon the cell types studied and the conditions used. In contrast to its transcriptional effects, the precise nongenomic signaling pathways of E2, especially the involvement of ERα in this process, are not well understood and have not been extensively studied (18–20).

Several recent reports demonstrated that E2 rapidly activates MAPK in a number of model systems (13, 21, 22), but the mechanisms responsible for this are still controversial (23–26). Many growth factor receptors on the cell membrane, such as the receptors for epidermal growth factor (27), nerve growth factor (28), platelet-derived growth factor (27), and IGF (29), activate MAPK through a Shc-mediated pathway. We hy-

Abbreviations: AF-1 and AF-2 domains, Activation function 1 and 2 domains; CH domain, collagen homology domain; EGFR, epidermal growth factor receptor; Grb2, growth factor receptor binding protein 2; GST, glutathione-*S*-transferase; HEGO, human ERα expression vector; ICI, ICI 182 780; IMEM, improved MEM; LTED cells, MCF-7 cells growing long-term in estrogen-depleted medium; MEK, MAPK kinase; PTB domain, phosphotyrosine binding domain; PVDF, polyvinylidene difluoride; Shc, Src-homology and collagen homology; ShcWT, wild-type Shc; Sos, Son of Sevenless; Src, Src family of tyrosine kinases; c-Src, p60 of Src.

pothesized that E2 might co-opt a pathway using Shc-Grb2-Sos (Src homology-growth factor receptor binding protein 2-son of sevenless) to activate MAPK. The adapter protein Shc has no intrinsic kinase domain and transduces signals dependent on the association with membrane receptors. Three domains mediating protein-protein interactions have been reported on Shc. Two of these, the phosphotyrosine binding (PTB) domain in the amino-terminal region and the Src homology 2 (SH2) domain in the carboxy-terminal region are separated by a region rich in proline and glycine residues, called the collagen homology (CH) domain (30). Shc binds rapidly to the specific phosphotyrosine residues of receptors through its PTB or SH2 domain and becomes phosphorylated itself on tyrosine residues of the CH domain (27). The phosphorylated tyrosine residues on the CH domain provide the docking sites for the binding of the SH2 domain of Grb2 and hence recruit Sos, a guanine nucleotide exchange protein. This adapter complex formation allows Ras activation via the Sos protein, leading to the activation of the MAPK pathway (27, 31, 32). Since ERα has been reported to be associated with the membrane of MCF-7 cells (20), we hypothesized that this receptor might be involved in mediating E2 action on MAPK activation by physical interaction with Shc in a manner analogous to that in growth factor pathways.

To test our hypothesis, we used MCF-7 and its variant LTED cells. LTED cells were developed from parental MCF-7 cells growing long-term in estrogen-depleted medium (33). This maneuver causes a 5- to 10-fold up-regulation of ERα expression (33). In the present study, we demonstrated that E2 rapidly stimulated both MAPK and Shc phosphorylation and induced the association of Shc with ERα. Using selective inhibitors and a dominant mutant Shc, we further demonstrated that Shc is upstream of MAPK and that the rapid actions of E2 are ERα-dependent and involve ERα/Shc association. Furthermore, a direct physical association of ERα with Shc was evidenced by protein pull-down assay. Our results show that the PTB and SH2 domains of Shc interacted with the AF-1 region of ERα. Tyrosine-537 of ERα was not involved in this interaction. Measurement of Elk-1 activation and morphological changes by confocal microscopy provided further evidence of the rapid, nongenomic role of E2 in these cells. Together, our data suggest that the nongenomic effects of E2 on Shc and MAPK activation are mediated by the classical ERα receptor, that E2 can induce an association of ERα with Shc, and that Shc appears to be a crucial step for the activation of MAPK.

RESULTS

Effects of Selective Inhibitors and Dominant-Negative Shc on E2-Induced MAPK Phosphorylation

Prior studies reported that E2 rapidly activated MAPK in MCF-7 cells (34). To investigate the upstream signals mediating E2 action on MAPK, we first confirmed that E2 increased MAPK activation in our MCF-7 cells by measuring MAPK phosphorylation. Figure 1A shows that E2 increased both p42 and p44 MAPK phosphorylation in a time-dependent manner with the peak at 15-min treatment. We then questioned

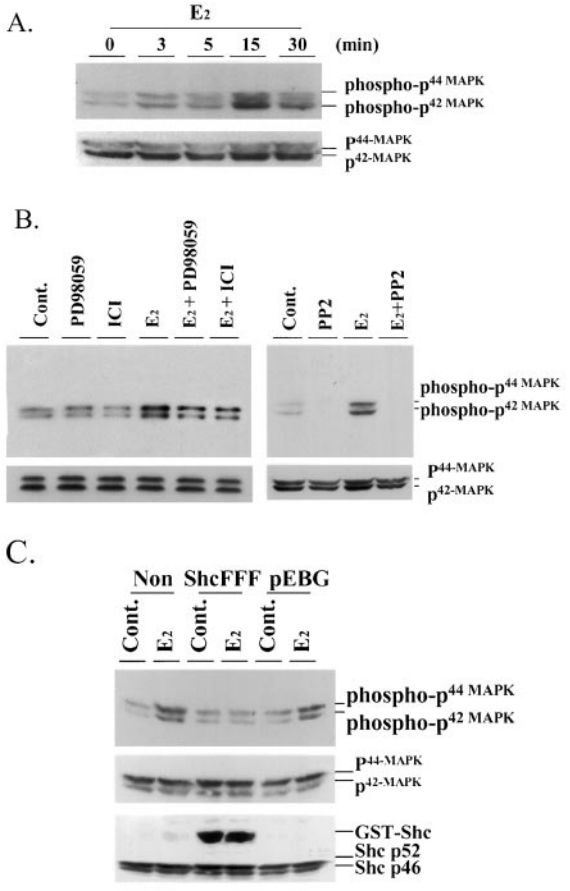

Fig. 1. MAPK Phosphorylation in MCF-7 Cells

A, E2-induced MAPK phosphorylation. MCF-7 cells were treated with vehicle or E2 at 10^{-10} M for the times indicated. The phosphorylation status of MAPK (p42 and p44) from whole-cell lysates was assessed using an antibody recognizing dual phosphorylated MAPK (*top panel*). Levels of total MAPK protein were determined on the same blot to control for loading variations (*bottom panel*). The positions of phosphorylated and total MAPK proteins are indicated at the *right*. B, Effects of pathway-selective inhibitors on E2-induced MAPK phosphorylation. MCF-7 cells were pretreated with 23 μM PD98059, 10^{-9} M ICI 182 780 (ICI), and 5 nM PP2 for 30 min. Cells were then treated with vehicle or 10^{-10} M E2 for 15 min. The phosphorylated (*top panel*) and total MAPK (*bottom panel*) were determined. C, Overexpression of mutant Shc blocked E2-induced MAPK phosphorylation. MCF-7 cells were either not transfected or transfected with the mutant Shc (ShcFFF) or control vectors (pEBG) for 2 d. Then cells were treated with vehicle or 10^{-10} M E2 for 15 min. The phosphorylated (*top panel*) and total MAPK (*middle panel*) were detected. Both GST-ShcFFF and endogenous Shc expression are shown (*bottom panel*). The above experiments have been repeated three times, and one of the representative experiments is shown.

whether the effects of E2 on MAPK involved ERα, MEK (MAPK kinase), and Src tyrosine kinase. As shown in Fig. 1B, the antiestrogen ICI, the MEK inhibitor PD98059, and a pan Src inhibitor PP2 all blocked E2-induced MAPK phosphorylation, implying that ERα, MEK, and Src family members are required for this step. PP2 alone abolished basal MAPK phosphorylation, suggesting the role of Src in maintaining basal MAPK function (Fig. 1B).

Activation of MAPK through classical growth factor signaling pathways involves the phosphorylation and activation of the adapter protein Shc. To test whether Shc is necessary for E2-induced MAPK phosphorylation, we transiently transfected MCF-7 cells with a dominant-negative Shc mutant. The mutant is a glutathione-*S*-transferase (GST) fusion protein with phenylalanines substituted for tyrosines at the 239/240 and 317 positions of the Shc CH domain (ShcFFF), rendering it defective in signaling to MAPK (35, 36). Expression of ShcFFF decreased E2-induced MAPK phosphorylation compared with untransfected and empty vector (pEBG)-transfected cells (Fig. 1C). Together, these results indicated that ERα, Src, and Shc are all upstream components regulating MAPK activation.

E2 Rapidly Induces Shc Pathway Activation

To further confirm the involvement of Shc in the E2 rapid signaling pathway, we evaluated this step in both MCF-7 and LTED cells that express a 10-fold elevation of ERα levels. As shown in the *top panel* of Fig. 2A, E2 at 10^{-10} M increased p52 kDa Shc phosphorylation in a time-dependent manner with the maximum response at 3 min. When LTED cells were compared with MCF-7 cells, Shc was phosphorylated to a greater extent in LTED cells (*left* in Fig. 2A) than parental MCF-7 cells (*right* in Fig. 2A) under basal conditions and increased proportionately in response to E2. To validate the results, the polyvinylidene difluoride (PVDF) membranes were reprobed with anti-Shc antibodies. The results show a similar amount of Shc proteins of both p46 and p52 kDa in MCF-7 and LTED cells (Fig. 2A, *bottom panels*). E2-induced Shc phosphorylation was also dose-dependent with the optimal dose at 10^{-10} M (data not shown).

Classical pathways of Shc activation by growth factors involve Shc association with the adapter proteins, Grb2 and Sos. Accordingly, we examined the effects of E2 on Shc-Grb2-Sos complex formation. LTED cells were used in this study because of their enhanced Shc phosphorylation in response to E2. As shown in Fig. 2B, Grb2/Shc (*left panel*) and Grb2/Sos (*middle* and *right panels*) complexes were faintly apparent in the vehicle-treated group, but greatly increased by 10^{-10} M E2 treatment at 3 min. Together, these results suggest that E2 is capable of activating the Shc-mediated signaling pathway in MCF-7 cells, which is regulated by the level of ERα expression.

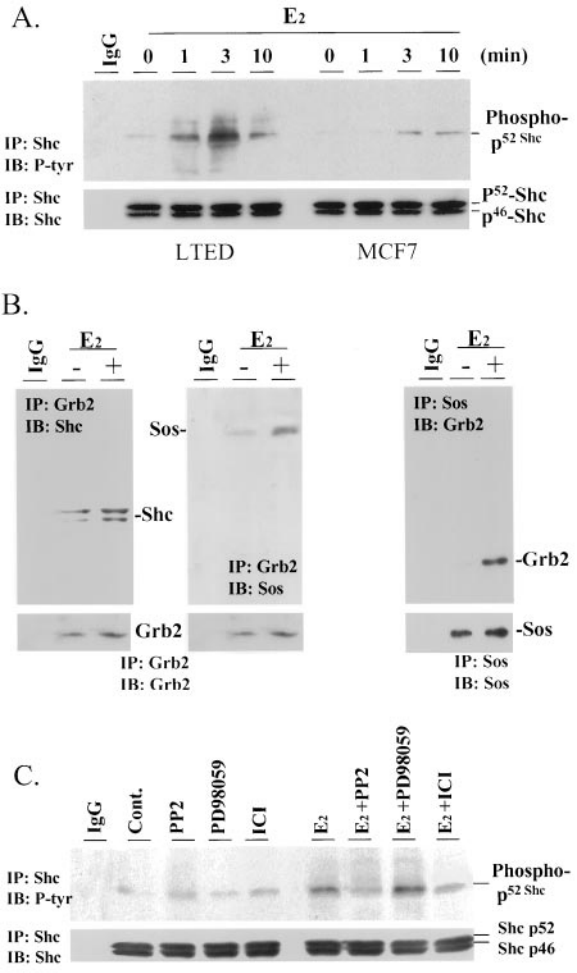

Fig. 2. E2-Induced Shc Pathway Activation in MCF-7 and Its Variant Cells

A, Effects of E2 on Shc phosphorylation. Both LTED and MCF-7 cells were treated with vehicle or 10^{-10} M E2 for the times indicated and then extracted as described in *Materials and Methods*. Shc phosphorylation was measured by immunoprecipitation (IP) of Shc protein and detection of tyrosine phosphorylation (*top panel*) on immunoblot (IB). To normalize Shc protein loading, the membranes were stripped and reprobed with polyclonal anti-Shc antibodies (*bottom panel*). Nonspecific monoclonal or polyclonal IgG were employed in all immunoprecipitation (IP) steps of the following experiments as negative controls. B, Effects of E2 on Shc-mediated adapter protein complex formation. LTED cells were treated with vehicle or E2 at 10^{-10} M for 3 min. The association of Grb2/Shc and Grb2/Sos was measured by immunoprecipitation of Grb2 and detection of Shc (*left top panel*) or Sos (*middle top panel*) on Western blots. The same membrane was reprobed with antibodies against Grb2 to detect Grb2 protein loading (*left* and *middle bottom panels*). The Grb2/Sos association was further confirmed by reciprocal antibody method (*right panel*). C, Effects of the selective inhibitors on E2-induced Shc phosphorylation in MCF-7 cells. MCF-7 cells were pretreated with 5 nM PP2, 23 μM PD98059, and 10^{-9} M ICI for 30 min. Cells then were challenged with vehicle or 10^{-10} M E2 for 3 min. The phosphorylation of Shc was determined as described in *Materials and Methods* (*top panel*). The membrane was reprobed with anti-Shc antibodies to show Shc protein loading (*bottom panel*). Above experiments were done three times and a representative experiment is shown.

Effects of Selective Signaling Pathway Inhibitors on E2-Induced Shc Phosphorylation

Because Shc is responsible for the activation of MAPK by E2, we wished to determine components responsible for Shc phosphorylation. Additionally, we wished to demonstrate a role for ERα in this process and to exclude MAPK as the cause of Shc phosphorylation. Shc has been reported to be a substrate of c-Src in HEK-293 cells (37). Accordingly, we examined the effects of PP2, ICI, and PD98059 on E2-induced Shc phosphorylation. In the presence of the inhibitors, MCF-7 cells were stimulated with vehicle or 10^{-10} M E2 for 3 min, and the status of Shc phosphorylation was examined. Figure 2C shows that both PP2 and ICI effectively inhibited E2-induced Shc phosphorylation, indicating that Src family kinases and ERα are required for Shc activation. As expected, PD98059 did not influence Shc phosphorylation status, suggesting that MAPK functions downstream of Shc. No effects of these inhibitors were apparent in the absence of E2 stimulation. These results indicate that both ERα and Src are upstream components of Shc functionality, and their involvement is required for Shc phosphorylation.

E2-Stimulated ERα Association with Shc

We postulated that ERα might mediate effects of E2 on Shc by directly or indirectly associating with the Shc adapter protein. This concept was based on the fact that activated Shc transduces signals by associating with membrane receptors and our evidence that ICI blocked E2-induced Shc phosphorylation in MCF-7 cells. To test this hypothesis, we immunoprecipitated Shc protein and detected ERα on Western blots. As shown in Fig. 3, E2 rapidly induced the association of ERα with Shc in both LTED and MCF-7 cells (*top panel*). The induction was seen as early as 1 min of E2 treatment and reached a plateau from 3 to 10 min. Compared with MCF-7 cells, ERα/Shc complexes were present basally in LTED cells, which express 5- to 10-fold higher levels of ERα, and greatly increased in response to E2 treatment. Consistency of protein loading was confirmed by reprobing the membrane with anti-Shc antibody (*bottom panel*). Thus, the association between ERα and Shc was observed not only in MCF-7 cells, but it was greatly enhanced in ERα up-regulated LTED cells. The results were also confirmed by the immunoprecipitation of ERα and the detection of Shc on immunoblot (data not shown). Together, our data suggest that as an upstream signal of Shc, the level of ERα expression affects the level of Shc phosphorylation and ERα/Shc association.

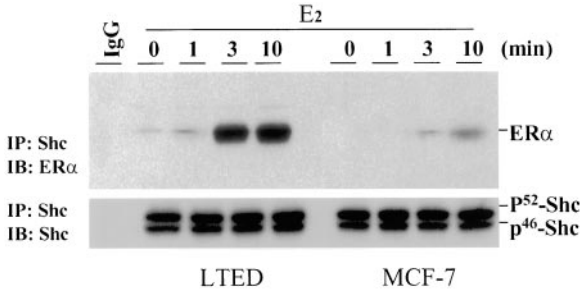

Fig. 3. E2 Rapidly Induced the Physical Association Between ERα and Shc in LTED and MCF-7 Cells

Cells were treated with vehicle or 10^{-10} M E2 for the times indicated. Subsequently, the association of ERα with Shc proteins was determined by the immunoprecipitation of Shc and detection of coimmunoprecipitated ERα protein on immunoblot (*top panel*). The same membrane was stripped and reprobed with anti-Shc antibodies to normalize the Shc protein loading (*bottom panel*). The positions of ERα and Shc proteins are indicated at the *right*. The experiment has been done three times, and one of the representative experiments is shown.

Study of Molecular Basis of ERα/Shc Interactions

To study the molecular basis of the interacting domains on ERα and Shc, various GST-tagged Shc and ERα mutants were employed (Fig. 4A). Furthermore, to minimize factors specific to breast cancer cells, COS-1 cells that do not have detectable endogenous ERα were used and electroporated with different ERα and Shc expressing vectors (Fig. 4A). First, we examined the Shc-interacting domain(s) on ERα by electroporating wild-type Shc (ShcWT) with either wild-type ERα expressing vector (HEGO) or a mutant ERα expressing vector in which phenylalanine was substituted for tyrosine in the 537-position (Y537F). As shown in Fig. 4B, the Y537F mutation did not alter the Shc/ERα complex formation compared with wild-type ERα, suggesting that Y537 of ERα is not the site interacting with Shc. Coexpression of either the truncated activation function 1 (AF-1) or activation function 2 (AF-2) domains of ERα with ShcWT in COS-1 cells confirmed that it is the AF-1, but not AF-2 (contains Y537), domain of ERα that interacts with Shc (Fig. 4, C and D). E2 increased the association of AF-1 with Shc (Fig. 4C). The mechanism for this is not known and was unexpected, since AF-1 does not contain a binding site for E2. We postulate that E2 might exert effects on AF-1 or Shc binding proteins independently of ERα, leading to an increase of AF-1/Shc association.

Next we further mapped the ERα-interacting site(s) on Shc. When ShcWT was coexpressed with ERα (HEGO) in COS-1 cells, we demonstrated an association of GST-Shc protein with ERα under basal conditions and further enhancement of this association with 5 min of E2 treatment (Fig. 4E, *top left panel*). We then used selective domain-expressing Shc mutants to examine which domains of Shc were necessary for this association. Both the PTB (ShcPTB)- and the SH2 (ShcSH2) domain-expressing proteins formed complexes with ERα, which further increased in intensity upon E2 stimulation (Fig. 4E, *top right panel*). Proteins that only expressed the GST or CH domain of Shc failed to interact with ERα. After normalizing the GST-Shc immunoprotein bands (Fig. 4E, *top panels*) for

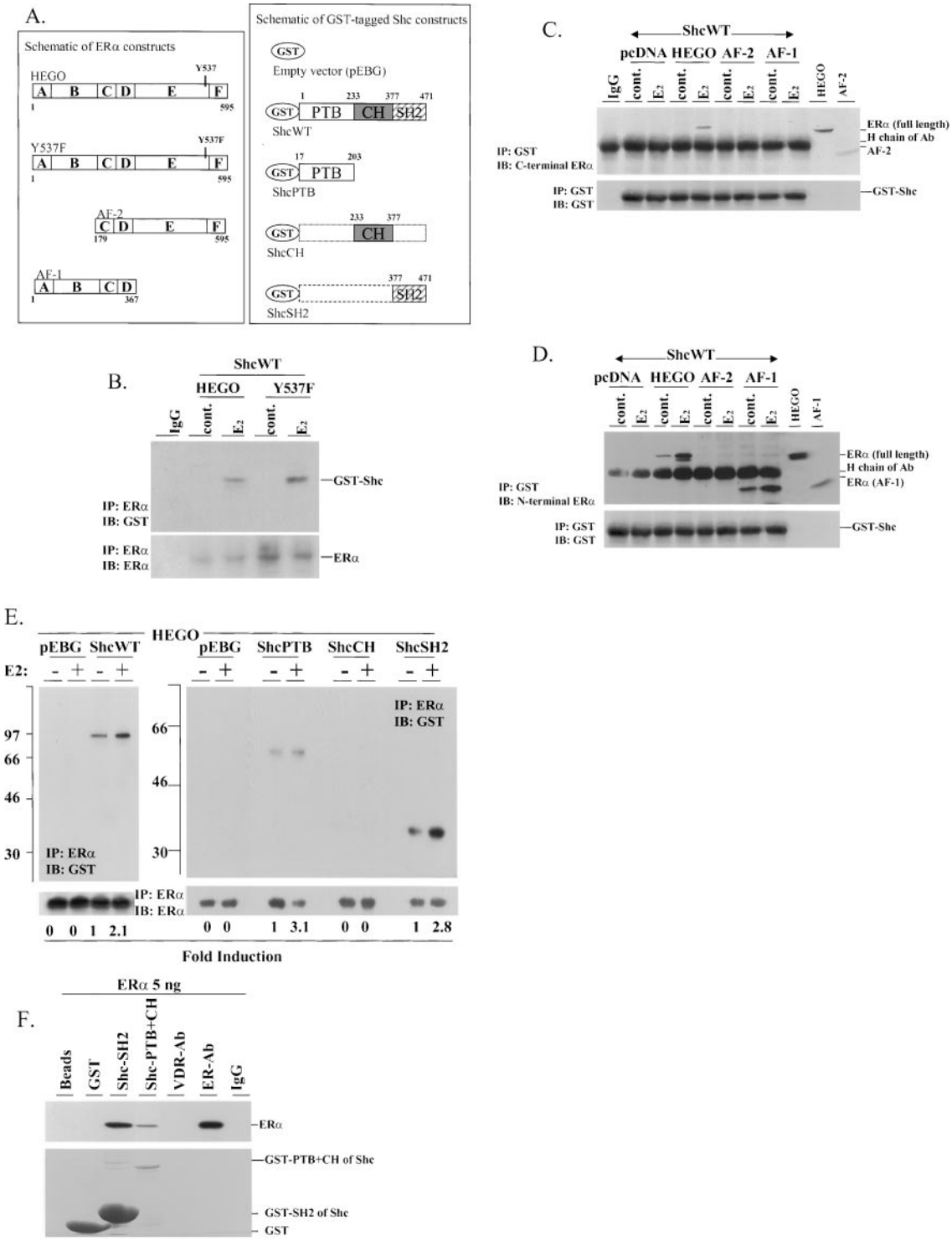

Fig. 4. Study of Shc/ERα Interaction

A, Schematic ERα and GST-tagged Shc constructs for eukaryotic expression. In *left panel*, HEGO is wild-type ERα-expressing vector. Y537F is a vector expressing mutant ERα in which the tyrosine-537 was mutated into phenylalanine. The AF-1 vector encodes amino acids 1–367 of ERα and AF-2 encodes 179–595. In the *right panel*, the GST-Shc fusion protein-expressing vectors are shown. The *oval region* in the N terminus of Shc corresponds to the GST fusion protein. The *white, gray*, and *diagonally lined rectangles* represent the PTB, CH, and SH2 domains of Shc, respectively. B, Examination of tyrosine-537 of ERα interaction with Shc. Wild-type Shc vector (ShcWT) was cotransfected with either HEGO or Y537F ERα-expressing vectors into COS-1 cells. Cells were then treated with vehicle or 10^{-10} M E2 for 5 min, and the ERα/Shc association was assessed. C and D, The AF-1 domain of ERα is required to interact with Shc. COS-1 cells were cotransfected with GST-tagged wild-type Shc (ShcWT) and different ERα constructs as indicated for 3 d. Cells were then treated with vehicle or 10^{-10} M E2 for 5 min. The ERα-Shc

ERα protein loading (Fig. 4E, *bottom panels*), we show that the Shc/ERα association induced by E2 is 2- to 3-fold higher than the control in cells expressing PTB or SH2 and is similar to that in cells containing ShcWT.

Shc can be a substrate of c-Src that associates with ERα in MCF-7 cells after E2 treatment (38). It would be of interest to know whether c-Src is involved in this ERα-Shc complex in our breast cancer system. Using several different anti-c-Src (B-12, N-16, and SRC2, Santa Cruz Biotechnology, Inc., Santa Cruz, CA) and anti-ERα antibodies (D-12 and MC-20, Santa Cruz Biotechnology, Inc.), we did not detect c-Src in ERα-Shc complexes of either MCF-7 or LTED cells (data not shown). To further address the molecular basis of Shc-ERα interaction, we tested whether this interaction is direct or mediated by third-party proteins using GST-pull-down assays. Both GST-tagged SH2 and PTH+CH domain fusion proteins of Shc were produced at the size of 37 kDa and 68 kDa (Fig. 4F, *bottom panel*). The 62-kDa recombinant full-length ERα was pulled down by both GST-tagged Shc proteins (Fig. 4F, *top panel*). As negative control, the beads and GST protein alone did not pull down the ERα protein. The specificity was confirmed by immunoprecipitation and detection of ERα with anti-ERα antibodies, but not by the nonspecific or anti-vitamin D receptor antibodies. Together, our results demonstrate that the interaction between ERα and Shc is direct and does not require the presence of any other proteins.

Biological Effects of E2-Induced Nongenomic Pathway Activation

To further provide evidence that the ERα-Shc-MAPK pathway is biologically relevant, we used two approaches. First, we evaluated the role of MAPK on the activation of Elk-1, which is a transcriptional factor phosphorylated and activated by MAPK (39). Second, we examined the rapid effects of E2 on morphological changes of MCF-7 cells.

To study Elk-1 activation by E2, a well characterized reporter system utilizing both GAL4-Elk-1 and GAL4-luciferase vectors (40) was cotransfected into MCF-7 cells. Figure 5 shows that E2 increased Elk-1 activation in a dose-dependent manner at 6 h as shown by luciferase assay. The E2 doses higher than 10^{-12} M significantly stimulated Elk-1 activation, indicating the involvement of MAPK in E2 action.

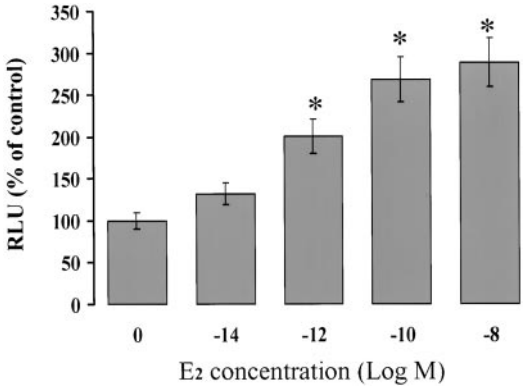

Fig. 5. E2-Stimulated MAPK Substrate Elk-1 Activation

A transient transfection method was used to study MAPK-mediated Elk-1 activation. MCF-7 cells were cotransfected with GAL4-Elk-1 and GAL4-E1B-Luciferase vectors. Twenty-four hours after transfection, cells were stimulated with vehicle or different doses of E2 for 6 h. Luciferase activity for each lysate was determined. The data are presented as mean ± SD of three experiments. *, $P < 0.05$ compared with untreated control.

To further provide direct biological evidence of E2 stimulation of Shc-MAPK pathways, effects of E2 on cell morphology were examined. We reasoned that E2 might elicit effects similar to those induced by exogenous growth factors since it used a pathway normally activated by growth factors, namely the Shc-MAPK pathway. Our coauthors recently used the confocal microscopic method to demonstrate that heregulin induces several rapid cellular effects, such as formation of membrane ruffles, filopodia, pseudopodia, actin polymerization, and loss of focal adhesion kinase plaques (41). Using identical methods, we studied rapid cell morphological changes and their substructures using LTED cells due to their strong responses

association (*top panels*) was measured by immunoprecipitation of GST and detection of ERα on immunoblot using either anti-C (panel C) or anti-N-terminal (panel D) ERα antibodies. The membrane was reprobed with anti-GST antibodies to normalize the protein loading (*bottom panels*). To confirm the positions of AF-1 and AF-2, the ER-transfected COS-1 cell extracts were loaded on the same gels, and the expression of immunoprotein bands of HEGO, AF-1, and AF-2 is shown on the *right sides* of the *top panels*. E, Mapping the ERα-interacting domains on Shc. Wild-type ERα (HEGO) was transiently transfected into COS-1 cells with different GST-tagged Shc expression vectors as indicated. On d 3, cells were extracted, and the interactions between ERα and wild-type Shc (*top left panel*) or mutated Shc proteins (*top right panel*) were measured as described in *Materials and Methods*. The same membranes were stripped and reprobed with anti-ERα antibody to normalize the protein loading (*bottom panels*). Quantitation of the GST-Shc immunoprotein bands normalized by ERα protein loading is shown as fold induction. All figures are representative blots of the study that was performed three times. F, GST pull-down assay of ERα-Shc interaction. GST-tagged fusion proteins expressing Shc-selective domains were purified by the beads of Glutathione Sepharose 4B. Beads (15 μl) conjugated with or without GST, GST-SH2, or GST-PTB+CH domains of Shc were incubated with 5 ng recombinant full-length human ERα protein overnight. To control the specificity, the full-length human ERα was also incubated with anti-vitamin D receptor, anti-ERα, or nonspecific immunoglobulin (IgG) as indicated. After washing the beads three times, the eluted proteins were resolved on 10% SDS-PAGE, transferred onto a PVDF membrane, and detected with anti-ERα antibody (*top panel*). The gel was stained with Coomassie blue to show the positions of the Shc fusion proteins (*bottom panel*). One of four experiments is shown.

with respect to ERα/Shc association and Shc phosphorylation upon E2 treatment.

Under basal conditions (Fig. 6A), LTED cells exhibited a low level of membrane ruffles (*red*), indicating minimal actin polymerization sites. ERα (*green*) appeared to be predominantly in the nucleus with some also present in the cytoplasm. Beginning at 10 min (data not shown) and increasing by 20 min, E2 induced dramatic morphological effects, including the formation of additional membrane ruffles and cell shape alterations (Fig. 6B). Even more dramatic was the formation of pseudopodia shown in Fig. 6C as an arm-like extension of the cell membrane with a fist-like structure at its terminus. To demonstrate that ERα mediated these morphological responses, the effects of E2 were abrogated by coadministration of the pure antiestrogen ICI along with E2 (Fig. 6D). ICI alone resulted in no morphological changes (Fig. 6E).

Use of confocal microscopy and immunofluorescence provided a dynamic means of assessing ERα location and alterations in response to E2. Accordingly, we focused on the region contiguous to the cell membrane. The *insets* in Fig. 6F show enlarged areas indicated by *arrows* in panels A–E. Under basal conditions, minimal *green* staining could be observed along the cell membrane of the cells (Fig. 6A, *inset a*, *right panel*). In marked contrast, E2 appeared to translocate ERα into the region along the membrane ruffles as indicated by the strong appearance of *green* staining (Fig. 6B, *inset b,right panel*). As shown by merging the *red* (actin) and *green* (ERα) views, the ERα appeared as *yellow* (Fig. 6B, *inset b, left panel*), indicating colocalization with actin in the membrane ruffles. Striking also was the translocation of the ERα into the fist-like region of the pseudopodia as shown by both the *green* staining (Fig. 6C, *inset c, right panel*) and *yellow* merged views (Fig. 6C, *inset c, left panel*). ICI blocked E2-induced ERα membrane translocation with little effect by it alone (Fig. 6, D and E; *inset d, right* and *left panels*; and *inset e, right* and *left panels*). The immunofluorescence staining

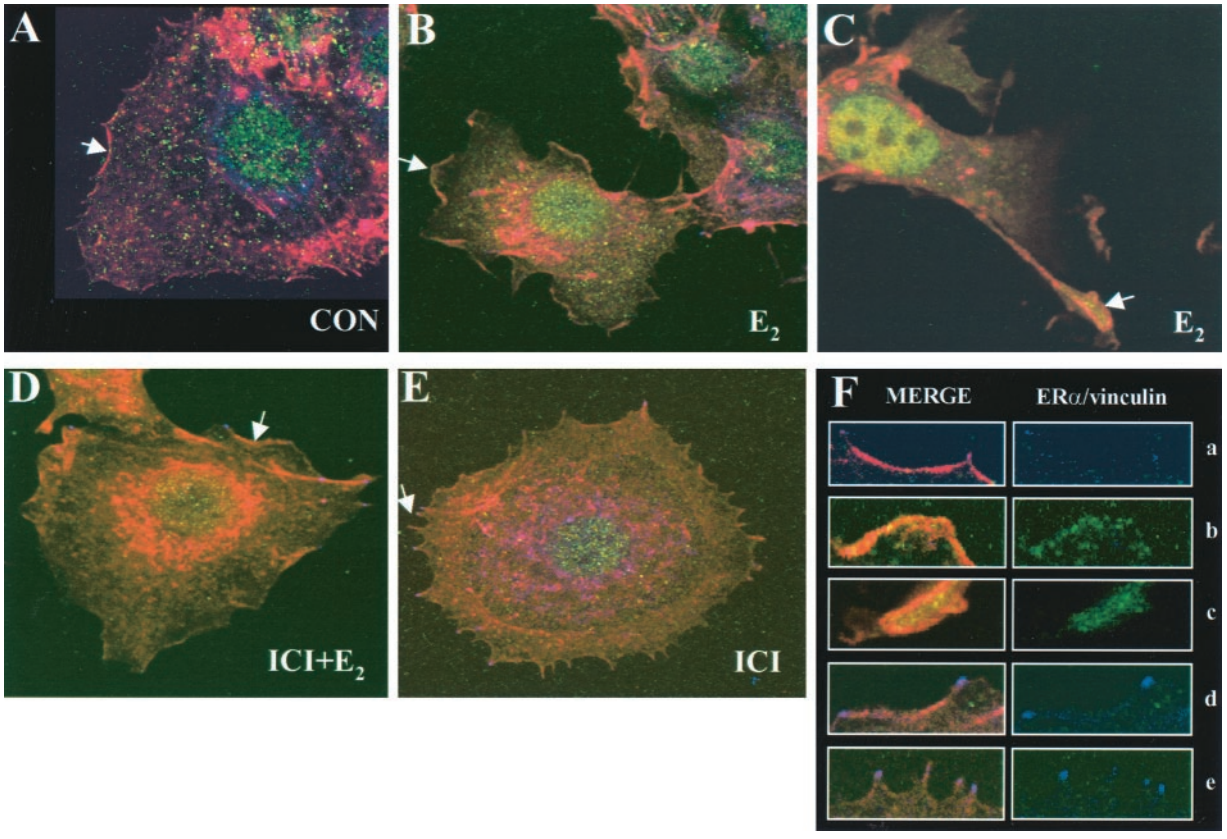

Fig. 6. Confocal Analysis of E2-Induced Morphological Changes and ERα Subcellular Localization in LTED Cells

Three-color-merged images are shown in panels A–E. *Red fluorescent color* indicates filamentous actin; *green* represents ERα; and *blue* indicates vinculin. Panel A illustrates cells grown under control conditions without E2. The *arrow* is directed toward a membrane ruffle that consists of concentrated bundles of filamentous actin. The regions indicated by the *arrow* in this and other panels (*i.e.* A–E) are further illustrated in the higher power views of specific areas shown as *insets* in panel F. Panel B illustrates cells treated with 10^{-10} M E2 for 20 min and shows the formation of additional membrane ruffles; panel C shows the formation of a pseudopodia under the same conditions. Panel D demonstrates that ICI at 10^{-9} M reduced the E2-induced ruffle formation, and panel E shows that ICI exerted no effect by itself. The *insets* in F represent the higher power views of specific areas of the membrane regions shown by *arrows* in panels A–E. On the *left panels* of the *insets* are shown the three-color ERα/filamentous actin/vinculin merged views; on the *right*, the two-color ERα/vinculin merged views are shown.

for vinculin (*blue*) represents the focal adhesion contacts of the cells that are not highly visible.

The morphological changes demonstrated in Fig. 6 represent examples of consistent changes observed in many cells. To establish that these changes were statistically significant, we used an integrated measure of membrane changes called dynamic membrane formation (DM). This integrated parameter includes both membrane ruffles and pseudopodia. As shown in Fig. 7, the E2-induced increase in DM was statistically significant and could be blocked by ICI. Collectively, these results demonstrated that E2 rapidly induced specific changes on cell morphology in addition to its effects on membrane-mediated Shc-MAPK activation.

DISCUSSION

Our studies demonstrated that MCF-7 breast cancer cells utilize a classical growth factor signaling pathway to mediate the nongenomic effects of E2. This pathway involves the direct association of ERα with Shc, the phosphorylation of Shc, and the formation of Shc-Grb2-Sos complexes. Shc is critical for E2-induced MAPK activation. Using a mutagenesis approach, we demonstrated that the SH2 and PTB domains of Shc are the sites interacting with ERα and that the AF-1 region of ERα is required to interact with Shc.

Evidence of the biological relevance of this pathway is inferred from the demonstration that Elk-1, one of the mediators of MAPK, was increased by E2. More importantly, we obtained direct biological evidence of the nongenomic effects of E2 by demonstrating morphological changes with confocal microscopy. These studies showed that E2 rapidly induced formation of membrane ruffles and pseudopodia, but also translocation of ERα to the membrane and into perimembrane regions of pseudopodia. Finally our results demonstrated that E2, mediated by ERα, activated a classical growth factor-signaling pathway involving Shc adapter proteins.

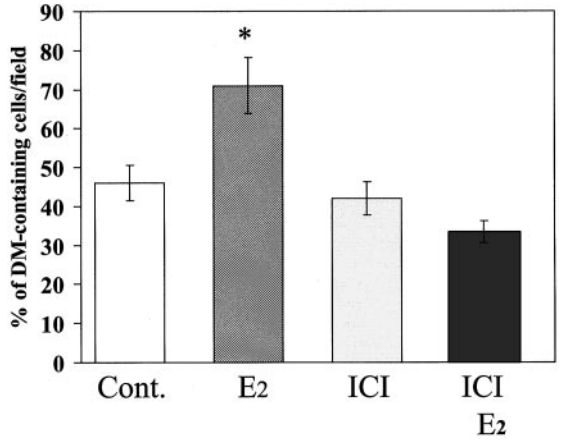

Fig. 7. Summary of Dynamic Membrane Formation in LTED Cells

The changes in ruffles and pseudopodias are combined under the term, dynamic membrane (DM), formation. Quantitative results from 12 individual cells are summarized. *, $P < 0.05$.

The adapter protein Shc mediates the effects of many growth factors to activate MAPK. However, several recent studies demonstrated different mechanisms whereby E2 can induce MAPK activation. McDonnell and associates (34) showed that calcium is required for E2-induced MAPK activation in MCF-7 cells, and this event is ERα dependent. E2-induced MAPK activation was also reported to be independent of ERα or ERβ but required the existence of epidermal growth factor receptor (EGFR) and GRP30, a G protein-coupled receptor homolog in an ERα-negative breast cancer cell line MDA-MB-231 (25). EGFR expression in MCF-7 cells is very low, and Parsons and colleagues (42) have reported that EGFR protein is not detectable in MCF-7 cells either by immunoprecipitation or by immunoblotting methods. In our system, we do not detect EGFR in either MCF-7 or its variant cells (data not shown).

In the present study, we demonstrated that ERα, as a key mediator, is required for E2 action on Shc/ERα association and Shc and MAPK phosphorylation. Approximately 0.5% of total ERα was estimated to be associated with Shc after E2 stimulation as shown by an ERα-Shc coimmunoprecipitation study (data not shown). The activation of MAPK with E2 is less than that by growth factors, as reported by other investigators (34). Our unpublished data also show that MAPK phosphorylation induced by 10 ng/ml TGFα was 35-fold higher than untreated controls, compared with 2.5-fold induction induced by 10^{-10} M E2. ERα-dependent MAPK activation has been reported by many laboratories using MCF-7 and other cell lines treated with E2 (39, 43). The differences regarding ERα involvement in MAPK activation under varying conditions are unknown. Nevertheless, it is not surprising that E2 can activate multiple rapid signaling pathways in different cell lines due to the fact that it can exert nongenomic effects on nitrous oxide, PKC, PKA, and MAPK. Detailed examination of E2 induction through each of these mechanisms will be required before a full understanding of the biological relevance of these various pathways emerges.

A single time point of Shc phosphorylation induced by E2 was first reported in MCF-7 cells (13). We extended these observations by conducting detailed time studies and showed the effects as early as 1 min after E2 treatment. ERα is required for Shc phosphorylation, and the association of ERα with Shc appears to be important for Shc activation. It has been suggested that PTB and SH2 are two distinct binding domains, which may link to phosphorylated tyrosine residues in a different manner (44). Both PTB and SH2 domains of Shc are required to associate with EGFR (45), but Neuregulin-activated ErbB2 and ErbB3 bind only to PTB domain of Shc (46). The functional roles of

the PTB or SH2 sites in their interaction with ERα are now under investigation.

The PTB and SH2 domains of Shc interact with phosphorylated tyrosine residue(s) of other proteins. The exact tyrosine residue of the ERα responsible for binding to Shc is unknown. Since tyrosine-537 of human ERα may serve as a constitutively phosphorylated site (7), we considered it a possible docking site for Shc. However, our data show that the AF-1 domain of ERα, but not the AF-2 or tyrosine-537 region, interacts with Shc, indicating that there might be other tyrosine residues phosphorylated on the N-terminal ERα. We postulated that 1 of 10 potential tyrosine residues in the AF-1 region (amino acids 1–179) might be involved in the association with Shc, such as tyrosine 43, 52, 54, 60, 73, 80, 130/131, 139, and 150. Further investigation of these sites is now being conducted in our laboratory.

ERα has been reported to associate functionally with many cell membrane proteins, such as IRS-1, the p85 subunit of PI3K, and caveolin (47–49). c-Src has been reported to physically associate with ERα of bovine uterus, but there is no direct evidence that ERα-associated c-Src is responsible for Shc phosphorylation (13). The present study demonstrated that the Src inhibitor PP2 blocked Shc phosphorylation induced by E2. This evidence suggests that a Src protein family member is functionally involved in E2-induced Shc phosphorylation, even though Src is not detectable in the ERα-Shc complex. It is possible that other Src family members are involved in phosphorylating Shc or that the Src-ERα complex is unstable during immunoprecipitation.

The breast cancer models used in our studies involve parental MCF-7 and its variant LTED cells. When compared with its parental cells, LTED cells show an increased growth rate in E2-deprived media and respond to very low concentrations of E2 when grown in nude mice (50). ERα, but not ERβ, is detectable in our MCF-7 and its variant cells (33, 50). The presence of increased amounts of ERα appears to amplify the components examined in the ERα-Shc signaling pathway. Whenever effects, such as ERα/Shc association and Shc phosphorylation, were compared in LTED and MCF-7 cells, the responses were qualitatively similar but quantitatively greater in the variants. For this reason, we used this variant for demonstrating certain effects such as Grb2/Sos interactions and morphological changes by confocal microscopy.

Our studies demonstrated rapid, nongenomic effects of E2 by two separate methods, biochemical assessment of the Shc-MAPK pathway and morphological effects on cell shape, membrane ruffles, pseudopodia, and ERα translocation. Both effects could be blocked by the antiestrogen ICI, indicating that Shc-MAPK activation and morphological changes were all initiated by ERα. Even though we do not yet have direct evidence that the observed E2 effects on cell structure are mediated by activation of the Shc and MAPK pathway, the role of Shc and MAPK on cell adhesion and motility has been demonstrated in several cell lines (51, 52). The interaction of Shc with membrane integrin in MCF-7 cells was reported to regulate the locomotion and cell adhesion of MCF-7 cells (53). We postulate that the E2-induced membrane signaling pathway activation, especially ERα-involved activation of Shc, might be linked to cell morphology changes in our cell models.

The suggestion that ERα can reside in or near the cell membrane has been controversial in the past (54). Recent transfection studies provided additional support that ERα can be present in the cell membrane (55). Razandi *et al.* (55) transfected ERα into Chinese hamster ovary (CHO) cells and demonstrated that 3% of expressed ERα was associated with cell membranes. Immunochemical studies with several anti-ERα antibodies on fixed cells including MCF-7 cells also suggested the presence of membrane ERα (20). Our observation using confocal microscopy showed that E2 increased the amounts of ERα in the region of the cell membrane. Our findings provide the first evidence that E2 can functionally influence the amount of ERα translocated into the perimembranous area. At the present time, we do not have direct morphological evidence that Shc is associated with this membrane-associated ERα, but we plan to examine this issue in the future.

In conclusion, we demonstrated that the signaling pathway mediating the rapid action of E2 involved the interaction of Shc with ERα, Shc activation, and the phosphorylation of MAPK. The PTB and SH2 domains of Shc as well as AF-1 domain of ERα are the sites mediating the interaction. Using selective pathway inhibitors and a dominant negative Shc mutant, we confirmed that ERα-mediated Shc activation resulted in MAPK phosphorylation in MCF-7 cells. As evidence of functionality, E2 rapidly stimulated cell morphological changes and induced activation of the MAPK substrate, Elk-1. Additional studies are now required to provide further proof of the role of each of the signaling molecules in the biological events observed.

MATERIALS AND METHODS

Reagents and Plasmids

Tissue culture supplies were obtained from Fisher Scientific (Pittsburgh, PA). Improved MEM (IMEM) with or without phenol red (zinc option, Richter's modification) and FBS were products of Life Technologies, Inc. (Gaithersburg, MD). E2 was obtained from Steraloids (Wilton, NH). ICI was from AstraZeneca, Inc. (Wilmington, DE). E2 and ICI were dissolved in ethanol with a final concentration of ethanol in medium of less than 0.01%. PP2 and PD98059 were from Calbiochem (La Jolla, CA) and dissolved in dimethylsulfoxide. Full-length ERα recombinant protein was purchased from Affinity BioReagents, Inc. (Golden, CO). Protease inhibitors, leupeptin, pepstatin, and aprotinin, were purchased from Sigma (St. Louis, MO).

Mammalian expression vectors encoding human 52-kDa forms or partial regions of Shc with GST fusion proteins were gifts from Dr. Ravichandran Kodi (University of Virginia, Charlottesville, VA) and have been described previously (46). The

amino acid sequences encoded by the different Shc constructs are: full-length (1–471), PTB (17–203), CH (233–377), and SH2 (377–471). The full-length human ERα expression vector (HEGO) was a gift from Dr. Rosalie Uht (University of Virginia) and has been previously reported (56). The ERα expression vectors of AF-1, AF-2, and the Y537F mutant in which tyrosine 537 was mutated into phenylalanine were constructed in our laboratory by PCR and site-directed mutagenesis (QuickChange, Stratagene, La Jolla, CA) as previously described (57). The fusion gene GAL4-Elk-1 and its reporter gene GAL4-E1B-Luc were generously provided by Dr. Michael J. Weber (University of Virginia) and have been described previously (40).

Cell Culture

The MCF-7 cells and COS-1 cells were maintained in 5% FBS-IMEM and 10% FBS-DMEM, respectively. The LTED cells were developed from MCF-7 cells by growing long term (*i.e.* 6 months to 2 yr) in phenol red-free IMEM supplemented with 5% Dextran-coated charcoal-stripped FBS and have been extensively characterized with respect to growth characteristics, responsiveness to E2, and ER content (33, 50). As determined by ligand binding assays as well as mRNA and Western blots, these cells contain 5- to 10-fold higher levels of endogenous ERα than the parental MCF-7 cells. The content of ERβ is negligible to absent as demonstrated by Western blot and PCR (data not shown). All cell lines were routinely cultured in a humidified 95% air-5% CO_2 incubator at 37 C.

Cell Stimulation and Lysate Preparation

For rapid E2-induced signaling pathway studies, cells cultured in IMEM containing 1% dextran-coated charcoal-stripped FBS were treated at 37 C with vehicle or E2. Time and doses are indicated in the figure legends. If inhibitors were used, cells were pretreated with the inhibitors for 30 min and then challenged with E2. Cells were washed once with ice-cold PBS containing 1 mM Na_2VO_4 and extracted with binding buffer (50 mM Tris, pH 8.0, 150 mM NaCl, 5 mM EDTA, 5% glycerol, 1% Triton X-100, 25 mM NaF, 2 mM Na_2VO_4, and 10 μg/ml of each aprotinin, leupeptin, and pepstatin). Cell lysates were centrifuged at 14,000 $\times$ *g* for 10 min at 4 C to pellet insoluble material. The supernatant of cell extract was analyzed for protein concentration by a DC protein assay kit based on the Lowry method (Bio-Rad Laboratories, Inc.).

Immunoprecipitation and Immunoblotting

Immunoprecipitation and immunoblotting were carried out as described previously (58). Briefly, 1 mg of cell lysate from each treatment was immunoprecipitated using one of the following antibodies: 1 μg monoclonal anti-Shc antibody (PG-797; Santa Cruz Biotechnology, Inc.), 1 μg monoclonal anti-ERα antibody (D-12, Santa Cruz Biotechnology, Inc.), 1.2 μg polyclonal anti-Grb2 antibody (C-23, Santa Cruz Biotechnology, Inc.), 1 μg polyclonal anti-GST antibody, and 1 μg monoclonal anti-Sos antibody (Transduction Laboratories, Inc., Lexington, KY). Incubations proceeded for 4 h at room temperature or overnight at 4 C in the presence of 35 μl of 50% slurry protein-G or protein-A Sepharose beads (Life Technologies, Inc.). The beads were washed three times in cold binding buffer. The proteins eluted from the beads were analyzed on 10% SDS-polyacrylamide gels and transferred to PVDF membranes. The PVDF membranes were probed with one of the following primary antibodies: horseradish peroxidase-conjugated monoclonal antiphosphotyrosine antibody (PY20, Transduction Laboratories, Inc.), polyclonal anti-ERα antibody (HC-20, Santa Cruz Biotechnology, Inc.), polyclonal anti-Shc (Transduction Laboratories, Inc.), polyclonal anti-GST antibodies (Z-5, Santa Cruz Biotechnology, Inc.), monoclonal anti-Grb2 (Transduction Laboratories, Inc.), monoclonal anti-GST, monoclonal anti-ERα N-terminal antibody (COIM2133, Fisher Scientific), polyclonal anti-C-terminal ERα antibodies (MC-20, Santa Cruz Biotechnology, Inc.), and polyclonal anti-Sos antibodies (Transduction Laboratories). After washing the PVDF membrane, the immunoblots were incubated with horseradish peroxidase-conjugated secondary antibodies for 1 h [donkey against rabbit IgG from Pierce Chemical Co. (Rockford, IL) or sheep against mouse IgG from Amersham Pharmacia Biotech (Piscataway, NJ)] and further developed using the chemiluminescence detection system (Pierce Chemical Co.). The reciprocal studies for all protein-protein interactions were conducted and the same results were confirmed. All experiments were done at least three times.

GST Pull-Down Assay

Prokaryotic vectors expressing both PTB+CH and SH2 domains of Shc were gifts from Dr. Ravichandran Kodi (University of Virginia), expressed in *Escherichia coli* BL21 and purified with a GST-glutathione affinity system (Amersham Pharmacia Biotech). GST, GST-ShcPTB+CH, and GST-ShcSH2 proteins were induced, solubilized, and bound to Glutathione beads. To test the protein interaction, 15 μl of the suspension were incubated in binding buffer with 5 ng of human full-length ERα expressed and purified from Baculovirus. After incubation, the beads were washed three times with the buffer. Bound proteins were eluted with 40 μl of 2$\times$ SDS-PAGE buffer, electrophoretically separated in 10% SDS gel, and transferred on the PVDF membrane. The membrane was probed with monoclonal anti-ERα antibody, and the immunoprotein bands were visualized as described above.

Electroporation and Transfection

COS-1 cells were electroporated exactly as described by Roy *et al.* (59) with 5 μg each of Shc constructs and 5 μg of each ERα-expressing vectors. Cells were then incubated in DMEM supplemented with 10% FBS for 48 h. The medium was changed again with serum-free and phenol-free DMEM for 1 d. Four hours before E2 treatment, the medium was changed again with fresh serum-free and phenol-free medium. Cells were then treated with E2 for 5 min and extracted with binding buffer. At this step, the samples were either stored at −80 C or prepared for protein-protein association assay. To study MAPK-mediated Elk-1 activation, MCF-7 cells were transiently transfected with both 2 ng of GAL4-Elk-1 and 0.1 μg of GAL4-E1B-Luc reporter vectors encoding GAL-Elk fusion protein and GAL-luciferase, respectively. Transfection was performed with Effectene transfection reagent (QIAGEN, Valencia, CA) according to company specifications; 24 h after transfection, cells were treated with different doses of E2 for 6 h. Luciferase activity was measured for each lysates, and samples were normalized by β-galactosidase cotransfected with above vectors. All transfections were conducted at least three times and the data are presented as mean $\pm$ SD.

Confocal Analysis of E2-Induced Cell Morphology Changes

Cells were fixed in paraformaldehyde followed by chilled acetone and blocked in normal goat serum followed by incubation with monoclonal antibody against vinculin (Sigma) and with polyclonal antibodies against ERα (Santa Cruz Biotechnology, Inc.). For triple costaining of filamentous actin, ERα and vinculin and 0.1 μM Alexa 546-conjugated phalloidin were included during incubation with the Alexa 633-goat antimouse and Alexa 488 goat antirabbit secondary antibodies. Slides were mounted, and analyzed by a LSM inverted microscope (Carl Zeiss, Thornwood, NY) (60). Each image

represents Z sections at the same cellular level and magnification. Confocal analysis was performed using a Carl Zeiss laser scanning confocal microscope and established methods, involving processing of the same section for each detector and comparing pixel by pixel. Localization of ERα with ruffles is demonstrated by the development of *yellow color* due to *red* and *green* overlapped pixels. The effect of E2 on the changes of filamentous actin in terms of dynamic membrane was measured based on the formation of ruffles and pseudopodia from 12 cells in each treatment. Extensive application of identical methods for analysis of effects of heregulin has been recently published by Adam *et al.* (41).

Acknowledgments

We thank Dr. Ravichandran Kodi for supplying the Shc-expressing constructs and Dr. Michael J. Weber for providing us with the Elk-1 vector. We also thank Dr. Rosalie Uht for her gift of ERα-expressing vector.

Received February 20, 2001. Accepted September 6, 2001.

Address all correspondence and requests for reprints to: Dr. Robert X. Song, Division of Hematology and Oncology, University of Virginia Health Science Center, Charlottesville, Virginia 22901. E-mail: rs5wf@virginia.edu.

This work was supported by NIH Grants CA-65622 (to R.J.S.), CA-80066 (to R.K.), and DK-57082 (to M.A.S.).

REFERENCES

1. Yager JD 2000 Endogenous estrogens as carcinogens through metabolic activation. J Natl Cancer Inst Monogr 27:67–73
2. Green S, Chambon P 1988 Nuclear receptors enhance our understanding of transcription regulation. Trends Genet 4:309–314
3. Chen D, Pace PE, Coombes RC, Ali S 1999 Phosphorylation of human estrogen receptor α by protein kinase A regulates dimerization. Mol Cell Biol 19:1002–1015
4. Chen D, Riedl T, Washbrook E, Pace PE, Coombes RC, Egly JM, Ali S 2000 Activation of estrogen receptor α by S118 phosphorylation involves a ligand-dependent interaction with TFIIH and participation of CDK7. Mol Cell 6:127–137
5. Joel PB, Smith J, Sturgill TW, Fisher TL, Blenis J, Lannigan DA 1998 pp90rsk1 Regulates estrogen receptor-mediated transcription through phosphorylation of Ser-167. Mol Cell Biol 18:1978–1984
6. Rogatsky I, Trowbridge JM, Garabedian MJ 1999 Potentiation of human estrogen receptor α transcriptional activation through phosphorylation of serines 104 and 106 by the cyclin A-CDK2 complex. J Biol Chem 274: 22296–22302
7. Arnold SF, Melamed M, Vorojeikina DP, Notides AC, Sasson S 1997 Estradiol-binding mechanism and binding capacity of the human estrogen receptor is regulated by tyrosine phosphorylation. Mol Endocrinol 11:48–53
8. Wang W, Dong L, Saville B, Safe S 1999 Transcriptional activation of E2F1 gene expression by 17β-estradiol in MCF-7 cells is regulated by NF-Y-Sp1/estrogen receptor interactions. Mol Endocrinol 13:1373–1387
9. Ziemiecki A, Catelli MG, Joab I, Moncharmont B 1986 Association of the heat shock protein hsp90 with steroid hormone receptors and tyrosine kinase oncogene products. Biochem Biophys Res Commun 138:1298–1307
10. Ying C, Lin DH, Sarkar DK, Chen TT 1999 Interaction between estrogen receptor and Pit-1 protein is influenced by estrogen in pituitary cells. J Steroid Biochem Mol Biol 68:145–152
11. Abbondanza C, Rossi V, Roscigno A, Gallo L, Belsito A, Piluso G, Medici N, Nigro V, Molinari AM, Moncharmont B, Puca GA 1998 Interaction of vault particles with estrogen receptor in the MCF-7 breast cancer cell. J Cell Biol 141:1301–1310
12. Migliaccio A, Piccolo D, Castoria G, Di Domenico M, Bilancio A, Lombardi M, Gong W, Beato M, Auricchio F 1998 Activation of the Src/p21ras/Erk pathway by progesterone receptor via cross-talk with estrogen receptor. EMBO J 17:2008–2018
13. Migliaccio A, Di Domenico M, Castoria G, de Falco A, Bontempo P, Nola E, Auricchio F 1996 Tyrosine kinase/p21ras/MAP-kinase pathway activation by estradiol-receptor complex in MCF-7 cells. EMBO J 15:1292–1300
14. Kelly MJ, Lagrange AH, Wagner EJ, Ronnekleiv OK 1999 Rapid effects of estrogen to modulate G protein-coupled receptors via activation of protein kinase A and protein kinase C pathways. Steroids 64:64–75
15. Beyer C, Karolczak M 2000 Estrogenic stimulation of neurite growth in midbrain dopaminergic neurons depends on cAMP/protein kinase A signalling. J Neurosci Res 59:107–116
16. Valverde MA, Rojas P, Amigo J, Cosmelli D, Orio P, Bahamonde MI, Mann GE, Vergara C, Latorre R 1999 Acute activation of Maxi-K channels by estradiol binding to the β subunit. Science 285:1929–1931
17. Stefano GB, Prevot V, Beauvillain JC, Cadet P, Fimiani C, Welters I, Fricchione GL, Breton C, Lassalle P, Salzet M, Bilfinger TV 2000 Cell-surface estrogen receptors mediate calcium-dependent nitric oxide release in human endothelia. Circulation 101:1594–1597
18. Collins P, Webb C 1999 Estrogen hits the surface. Nat Med 5:1130–1131
19. Watson CS, Campbell CH, Gametchu B 1999 Membrane oestrogen receptors on rat pituitary tumour cells: immuno- identification and responses to oestradiol and xenoestrogens. Exp Physiol 84:1013–1022
20. Watson CS, Norfleet AM, Pappas TC, Gametchu B 1999 Rapid actions of estrogens in GH3/B6 pituitary tumor cells via a plasma membrane version of estrogen receptor-α. Steroids 64:5–13
21. Bi R, Broutman G, Foy MR, Thompson RF, Baudry M 2000 The tyrosine kinase and mitogen-activated protein kinase pathways mediate multiple effects of estrogen in hippocampus. Proc Natl Acad Sci USA 97:3602–3607
22. Neugarten J, Medve I, Lei J, Silbiger SR 1999 Estradiol suppresses mesangial cell type I collagen synthesis via activation of the MAP kinase cascade. Am J Physiol 277:F875–F881
23. Singh M, Setalo Jr G, Guan X, Frail DE, Toran-Allerand CD 2000 Estrogen-induced activation of the mitogen-activated protein kinase cascade in the cerebral cortex of estrogen receptor-α knock-out mice. J Neurosci 20: 1694–1700
24. Kuroki Y, Fukushima K, Kanda Y, Mizuno K, Watanabe Y 2000 Putative membrane-bound estrogen receptors possibly stimulate mitogen-activated protein kinase in the rat hippocampus. Eur J Pharmacol 400:205–209
25. Filardo EJ, Quinn JA, Bland KI, Frackelton Jr AR 2000 Estrogen-induced activation of Erk-1 and Erk-2 requires the G protein-coupled receptor homolog, GPR30, and occurs via trans-activation of the epidermal growth factor receptor through release of HB-EGF. Mol Endocrinol 14: 1649–1660
26. Castoria G, Barone MV, Di Domenico M, Bilancio A, Ametrano D, Migliaccio A, Auricchio F 1999 Non-transcriptional action of oestradiol and progestin triggers DNA synthesis. EMBO J 18:2500–2510
27. Pelicci G, Lanfrancone L, Salcini AE, Romano A, Mele S, Grazia BM, Segatto O, Di Fiore PP, Pelicci PG 1995

Constitutive phosphorylation of Shc proteins in human tumors. Oncogene 11:899–907
28. Dikic I, Batzer AG, Blaikie P, Obermeier A, Ullrich A, Schlessinger J, Margolis B 1995 Shc binding to nerve growth factor receptor is mediated by the phosphotyrosine interaction domain. J Biol Chem 270:15125–15129
29. Ishihara H, Sasaoka T, Wada T, Ishiki M, Haruta T, Usui I, Iwata M, Takano A, Uno T, Ueno E, Kobayashi M 1998 Relative involvement of Shc tyrosine 239/240 and tyrosine 317 on insulin induced mitogenic signaling in rat1 fibroblasts expressing insulin receptors. Biochem Biophys Res Commun 252:139–144
30. Pelicci G, Dente L, De Giuseppe A, Verducci-Galletti B, Giuli S, Mele S, Vetriani C, Giorgio M, Pandolfi PP, Cesareni G, Pelicci PG 1996 A family of Shc related proteins with conserved PTB, CH1 and SH2 regions. Oncogene 13:633–641
31. Blenis J 1993 Signal transduction via the MAP kinases: proceed at your own RSK. Proc Natl Acad Sci USA 90:5889–5892
32. Boney CM, Gruppuso PA, Faris RA, Frackelton Jr AR 2000 The critical role of Shc in insulin-like growth factor-I-mediated mitogenesis and differentiation in 3T3-L1 preadipocytes. Mol Endocrinol 14:805–813
33. Jeng MH, Shupnik MA, Bender TP, Westin EH, Bandyopadhyay D, Kumar R, Masamura S, Santen RJ 1998 Estrogen receptor expression and function in long-term estrogen-deprived human breast cancer cells. Endocrinology 139:4164–4174
34. Improta-Brears T, Whorton AR, Codazzi F, York JD, Meyer T, McDonnell DP 1999 Estrogen-induced activation of mitogen-activated protein kinase requires mobilization of intracellular calcium. Proc Natl Acad Sci USA 96:4686–4691
35. Pratt JC, van den Brink MR, Igras VE, Walk SF, Ravichandran KS, Burakoff SJ 1999 Requirement for Shc in TCR-mediated activation of a T cell hybridoma. J Immunol 163:2586–2591
36. Ravichandran KS, Lorenz U, Shoelson SE, Burakoff SJ 1995 Interaction of Shc with Grb2 regulates the Grb2 association with mSOS. Ann NY Acad Sci 766:202–203
37. Sato KI, Kimoto M, Kakumoto M, Horiuchi D, Iwasaki T, Tokmakov AA, Fukami Y 2000 Adaptor protein shc undergoes translocation and mediates up-regulation of the tyrosine kinase c-Src in EGF-stimulated A431 cells. Genes Cells 5:749–764
38. Migliaccio A, Castoria G, Di Domenico M, de Falco A, Bilancio A, Lombardi M, Barone MV, Ametrano D, Zannini MS, Abbondanza C, Auricchio F 2000 Steroid-induced androgen receptor-oestradiol receptor β-Src complex triggers prostate cancer cell proliferation. EMBO J 19:5406–5417
39. Duan R, Xie W, Safe S 2001 Estrogen receptor-mediated activation of the serum response element in MCF-7 cells through MAPK-dependent phosphorylation of Elk-1. J Biol Chem 276:11590–11598
40. Roberson MS, Misra-Press A, Laurance ME, Stork PJ, Maurer RA 1995 A role for mitogen-activated protein kinase in mediating activation of the glycoprotein hormone α-subunit promoter by gonadotropin-releasing hormone. Mol Cell Biol 15:3531–3539
41. Adam L, Vadlamudi R, Kondapaka SB, Chernoff J, Mendelsohn J, Kumar R 1998 Heregulin regulates cytoskeletal reorganization and cell migration through the p21-activated kinase-1 via phosphatidylinositol-3 kinase. J Biol Chem 273:28238–28246
42. Biscardi JS, Belsches AP, Parsons SJ 1998 Characterization of human epidermal growth factor receptor and c-Src interactions in human breast tumor cells. Mol Carcinog 21:261–272
43. Watters JJ, Chun TY, Kim YN, Bertics PJ, Gorski J 2000 Estrogen modulation of prolactin gene expression requires an intact mitogen-activated protein kinase signal transduction pathway in cultured rat pituitary cells. Mol Endocrinol 14:1872–1881
44. Cattaneo E, Pelicci P 1998 Emerging roles for SH2/PTB-containing Shc adapter proteins in the developing mammalian brain. Trends Neurosci 21:476–481
45. Batzer AG, Rotin D, Urena JM, Skolnik EY, Schlessinger J 1994 Hierarchy of binding sites for Grb2 and Shc on the epidermal growth factor receptor. Mol Cell Biol 14: 5192–5201
46. Won S, Si J, Colledge M, Ravichandran KS, Froehner SC, Mei L 1999 Neuregulin-increased expression of acetylcholine receptor ϵ-subunit gene requires ErbB interaction with Shc. J Neurochem 73:2358–2368
47. Simoncini T, Hafezi-Moghadam A, Brazil DP, Ley K, Chin WW, Liao JK 2000 Interaction of oestrogen receptor with the regulatory subunit of phosphatidylinositol-3-OH kinase. Nature 407:538–541
48. Schlegel A, Wang C, Katzenellenbogen BS, Pestell RG, Lisanti MP 1999 Caveolin-1 potentiates estrogen receptor α (ERα) signaling: Caveolin-1 drives ligand-independent nuclear translocation and activation of ERα. J Biol Chem 274:33551–33556
49. Kahlert S, Nuedling S, van Eickels M, Vetter H, Meyer R, Grohe C 2000 Estrogen receptor α rapidly activates the IGF-1 receptor pathway. J Biol Chem 275:18447–18453
50. Masamura S, Santner SJ, Heitjan DF, Santen RJ 1995 Estrogen deprivation causes estradiol hypersensitivity in human breast cancer cells. J Clin Endocrinol Metab 80: 2918–2925
51. Imai Y, Clemmons DR 1999 Roles of phosphatidylinositol 3-kinase and mitogen-activated protein kinase pathways in stimulation of vascular smooth muscle cell migration and deoxyriboncleic acid synthesis by insulin-like growth factor-I. Endocrinology 140:4228–4235
52. Gu J, Tamura M, Pankov R, Danen EH, Takino T, Matsumoto K, Yamada KM 1999 Shc and FAK differentially regulate cell motility and directionality modulated by PTEN. J Cell Biol 146:389–403
53. Mauro L, Sisci D, Bartucci M, Salerno M, Kim J, Tam T, Guvakova MA, Ando S, Surmacz E 1999 SHC-α5β1 integrin interactions regulate breast cancer cell adhesion and motility. Exp Cell Res 252:439–448
54. Levin ER 1999 Cellular functions of the plasma membrane estrogen receptor. Trends Endocrinol Metab 10:374–377
55. Razandi M, Pedram A, Greene GL, Levin ER 1999 Cell membrane and nuclear estrogen receptors (ERs) originate from a single transcript: studies of ERα and ERβ expressed in Chinese hamster ovary cells. Mol Endocrinol 13:307–319
56. Webb P, Nguyen P, Valentine C, Lopez GN, Kwok GR, McInerney E, Katzenellenbogen BS, Enmark E, Gustafsson JA, Nilsson S, Kushner PJ 1999 The estrogen receptor enhances AP-1 activity by two distinct mechanisms with different requirements for receptor transactivation functions. Mol Endocrinol 13:1672–1685
57. Resnick EM, Schreihofer DA, Periasamy A, Shupnik MA 2000 Truncated estrogen receptor product-1 suppresses estrogen receptor transactivation by dimerization with estrogen receptors α and β. J Biol Chem 275:7158–7166
58. Harmer SL, DeFranco AL 1999 The src homology domain 2-containing inositol phosphatase SHIP forms a ternary complex with Shc and Grb2 in antigen receptor-stimulated B lymphocytes. J Biol Chem 274:12183–12191
59. Roy S, Lane A, Yan J, McPherson R, Hancock JF 1997 Activity of plasma membrane-recruited Raf-1 is regulated by Ras via the Raf zinc finger. J Biol Chem 272: 20139–20145
60. Adam L, Vadlamudi R, Mandal M, Chernoff J, Kumar R 2000 Regulation of microfilament reorganization and invasiveness of breast cancer cells by kinase dead p21-activated kinase-1. J Biol Chem 275:12041–12050